Int J Adv Manuf Technol (2011) 54:195–201
DOI 10.1007/s00170-010-2924-8

ORIGINAL ARTICLE

Characteristics of and measurement methods for geometric errors in CNC machine tools

Huanlao Liu · Bing Li · Xiaozheng Wang · Guangyu Tan

Received: 13 March 2009 / Accepted: 26 August 2010 / Published online: 14 September 2010
© Springer-Verlag London Limited 2010

Abstract The characteristics of geometric errors in CNC machine tools have been investigated in detail. These characteristics include position dependence, relativity, synthesis, and continuity. Tests have been designed to verify these properties, which can be used to guide the error measurement procedure. A new measurement procedure, called the relay method, has been developed. This method has high resolution and can be applied to measure geometric errors in the whole workspace. A machine has been calibrated by the relay method, and the results of error compensation show that the machine tool accuracy has been improved.

Keywords CNC machine tools · Geometric error · Error characteristics · Error measurement

1 Introduction

Geometric and thermally induced errors account for about 70% of the errors in machine tools. Therefore, compensation for geometric and thermal errors could significantly enhance the accuracy of machine tools and then improve the quality of parts produced with them [1, 2]. The geometric errors are those errors that exist in a machine on account of its basic design, and those resulting from the inaccuracies built in during assembly and from the components used in the machine. Geometric errors make up the major part of the inaccuracy of a machine tool [3]. As such, they form one of the biggest sources of inaccuracy in the parts produced. Geometric errors are systematic, or repeatable, and can be measured and stored; compensatory actions are effective. Accurate error prediction is one of the most important steps in the whole compensation procedure.

A laser interferometer is commonly used in the measurement of the various components of the errors. It has the disadvantage that the method needs an expert operator and a long measurement time, and it is not suitable for actual industrial application [4]. A double ball-bar can be used for checking the errors when the machine is moving in a circle [5]. The results can usually be used for periodic checking. Hua, Yanbin and Yan [6] proposed a two-link method which can be used to map errors in two dimensions, and identified the trajectory errors of general planar motions. A telescopic ball-bar can be used to enlarge the measurement area; Shih-Ming and Ehmann [7, 8] suggested the use of a triangulation principle and a single-socket method. These methods can, theoretically, detect position errors in a volume. However, they are usually very time-consuming and labor-intensive when used to calibrate a machine.

A cross-grid encoder can measure the two-dimensional error in a small area of a planar table [9]. The most commonly used cross-grid encoder is 220 mm in diameter, making it unusable for error detection in the whole volume of a workspace. Though current instrumentation permits the precise measurement of deviations from accurate geometry, simpler and less expensive methods are highly desirable. This paper provides a relay method to measure volumetric

H. Liu (✉) · X. Wang · G. Tan
Engineering Training Center, Guangdong Ocean University,
Zhanjiang, Guangdong 524025, China
e-mail: huanlao_liu@hotmail.com

B. Li
National CNC Control Research Center,
Huazhong University of Science and Technology,
Wuhan 430074, China

errors in a plane. Using equipment such as a cross-grid encoder that can measure in only a small field, the errors are obtained over the whole workspace by measuring the error in a basic position near the original point. Section 2 discusses in detail the characteristics of geometric errors in computed numerically controlled (CNC) machine tools. Some experimental procedures for measuring these characteristics are provided in Section 3. In Section 4, some results of error compensation are given. Finally, our conclusions are given in Section 5.

2 The characteristics of geometric errors

Geometric errors are those errors that are concerned with the quasi-static accuracy of surfaces moving relative to one another. Although better performance can be reached by improving the design and production of a machine, the achievable accuracy is still limited because of the limitations imposed by the physical properties of the materials and economic concerns. An effective method of compensation for these errors which includes both error prediction and a compensation system is needed.

2.1 Problem statement

The geometric errors are affected by factors such as surface straightness, surface roughness, and bearing preload. The geometric errors are always repeatable and time-invariant. The following experiments conditions are considered in the analysis.

1. Only those errors that represent a change in the basic accuracy of the geometric errors are considered, and not those that are process-dependent, such as the effects of temperature and of the cutting force.
2. The influence of backlash error has been eliminated before the tests; that is, the backlash in the axes has been well compensated by software or hardware methods.

2.2 Position dependence

As Fig. 1 shows, the magnitudes of the position coordinates of a commanded point ***P*** in the workspace can be expressed as $P = (xi + yj + zk)$. When the machine is commanded to move from point ***O*** to point ***P***, the actual (real) point $\boldsymbol{P_r}$ reached can be expressed as $P_r = (x_r i + y_r j + z_r k)$, and then the error in the commanded point ***P*** is $E = (E_x i + E_y j + E_z k)$. The error can be defined as $E = P_r - P + \varepsilon$, where $\varepsilon = (\varepsilon_x i + \varepsilon_y j + \varepsilon_z K)$ is the random error. The systematic error is the main error in soft compensation. The random error is not considered here, and

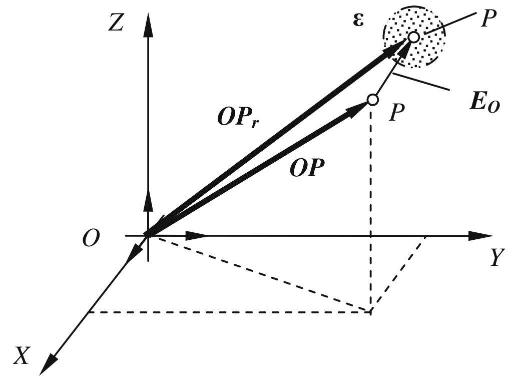

Fig. 1 Position dependence of position error

so the error can be described by $E = P_r - P$, and the equation for it can be expressed in detail as follows:

$$E_x = x - x_{r.},\ E_y = y - y_{r.},\ E_z = z - z_r \tag{1}$$

The geometric error ***E*** is the end-effect error, which can be described as a function of the point ***P***. So the error ***E*** can also be called the position-dependence error. The trajectory, and the direction of the error measurement under special conditions, can be ignored. This is the basic theory of out-of-line error compensation.

2.3 Relativity

The position error is illustrated further in Fig. 2. When the machine moves from point ***A*** to point ***P***, the real linear movement distance is $\boldsymbol{AP_r}$ and the commanded linear movement distance is ***AP***, and so the error is described by $E_{AP} = AP_r - AP$. The position error $\boldsymbol{E_{AP}}$ can be acquired by subtracting the commanded movement ***AP*** from the actual movement $\boldsymbol{AP_r}$. The error of the reference point ***A*** is considered as zero, i.e., $E(A) = E_{AA} = \mathbf{0}$.

As mentioned above, the position error implies a reference point, and the value of the position error is given relative to that reference point. This is the characteristic of relativity of position error.

2.4 Synthesis

As Fig. 3 shows, the original point on the working table *XOY* is ***O*** and the error of the original point ***O*** is ***E***(***O***)=0.

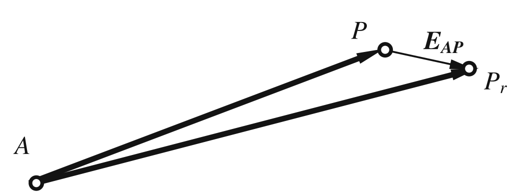

Fig. 2 Relativity of position error

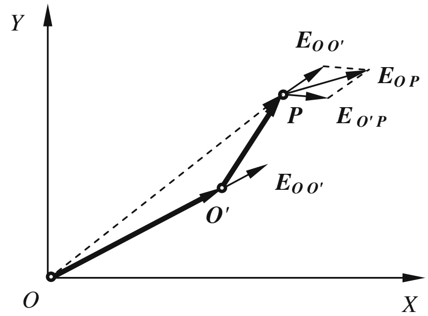

Fig. 3 Synthesis of position errors

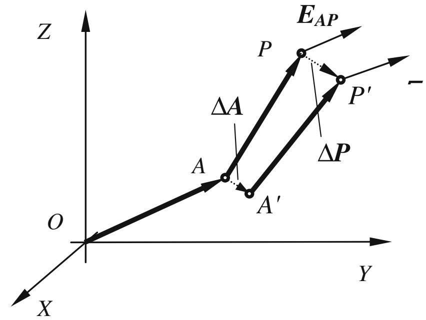

Fig. 5 Continuity of position error

The geometric error of the point $\boldsymbol{O'}$ is $\boldsymbol{E_{OO'}}$. The error of point $\boldsymbol{P}$ relative to point $\boldsymbol{O'}$ can be described by $\boldsymbol{E_{O'P}}$, and then the commanded linear movement distance is $OP = OO' + O'P$ and the actual linear movement distance is $OP_r = OO'_r + O'P_r$. Therefore, the error can be derived from the equation $E_{op} = OP_r - OP = (OO'_r + O'P_r) - (OO' + O'P) = (OO'_r - OO') + (\mathrm{O}'P_r - \mathrm{O}'P)$, and so $E_{OP} = E_{OO'} + E_{O'P}$.

The above equations demonstrate that the error of point $\boldsymbol{P}$ can be obtained from the error relative to the point $\boldsymbol{O'}$. These equations can be developed further to measure the error of a point $\boldsymbol{Q}$ (not shown in the figure). For example, the error $\boldsymbol{E_{PQ}}$, which is the error of point $\boldsymbol{Q}$ relative to point $\boldsymbol{P}$, can be measured, so the error $\boldsymbol{E_{OQ}}$ can be obtained from the equation $E_{OQ} = E_{OO'} + E_{O'P} + E_{PQ}$.

Generally, if the linear movements have the relationship $OP = OA + AB + BC + CD + \ldots + XP$, as shown in Fig. 4, the position error can be synthesized from the following equation: $E_{OP} = E_{OA} + E_{AB} + E_{BC} + E_{CD} + \ldots + E_{XP}$.

2.5 Continuity

A slight variation of the commanded movement $\Delta\boldsymbol{P}$ can lead to the actual error $\Delta\boldsymbol{E_P}$ also having a slight variation. Furthermore, a slight variation $\Delta\boldsymbol{A}=\boldsymbol{AA'}$ or $\Delta\boldsymbol{P}=\boldsymbol{PP'}$ of the commanded reference point $\boldsymbol{A}$ or of the end point $\boldsymbol{P}$ can cause a slight variation of the error $\Delta\boldsymbol{E_{AP}}$, as shown in Fig. 5:

$$E_{A'P'} = E_{AP} + \frac{\partial E}{\partial A} dA + \frac{\partial E}{\partial P} dP \tag{2}$$

So,

$$\Delta E_{AP} = E_{A'P'} - E_{AP} = \frac{\partial E}{\partial A} dA + \frac{\partial E}{\partial P} dP \tag{3}$$

Here, d$\boldsymbol{A}$ and d$\boldsymbol{P}$ can be expressed as follows:

$$dA = \begin{bmatrix} \mathrm{d}A_x \\ \mathrm{d}A_y \\ \mathrm{d}A_z \end{bmatrix}, \quad \mathrm{d}P = \begin{bmatrix} \mathrm{d}P_x \\ \mathrm{d}P_y \\ \mathrm{d}P_z \end{bmatrix} \tag{4}$$

and

$$\frac{\partial E}{\partial A} = \begin{bmatrix} \frac{\partial E_x}{\partial A_x} & \frac{\partial E_x}{\partial A_y} & \frac{\partial E_x}{\partial A_z} \\ \frac{\partial E_y}{\partial A_x} & \frac{\partial E_y}{\partial A_y} & \frac{\partial E_y}{\partial A_z} \\ \frac{\partial E_z}{\partial A_x} & \frac{\partial E_z}{\partial A_y} & \frac{\partial E_z}{\partial A_z} \end{bmatrix}, \quad \frac{\partial E}{\partial P} = \begin{bmatrix} \frac{\partial E_x}{\partial P_x} & \frac{\partial E_x}{\partial P_y} & \frac{\partial E_x}{\partial P_z} \\ \frac{\partial E_y}{\partial P_x} & \frac{\partial E_y}{\partial P_y} & \frac{\partial E_y}{\partial P_z} \\ \frac{\partial E_z}{\partial P_x} & \frac{\partial E_z}{\partial P_y} & \frac{\partial E_z}{\partial P_z} \end{bmatrix} \tag{5}$$

When d$\boldsymbol{A}$ and d$\boldsymbol{P}$ are small, the position error $\Delta\boldsymbol{E_{AP}}$ is also very small. Shih-Ming and Ehmann [8] also state the assumption that points located close to each other within a small volume exhibit the same position error.

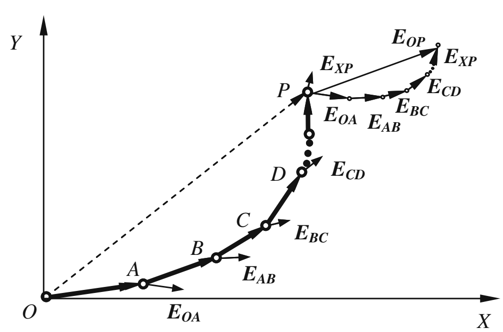

Fig. 4 General synthesis of position errors

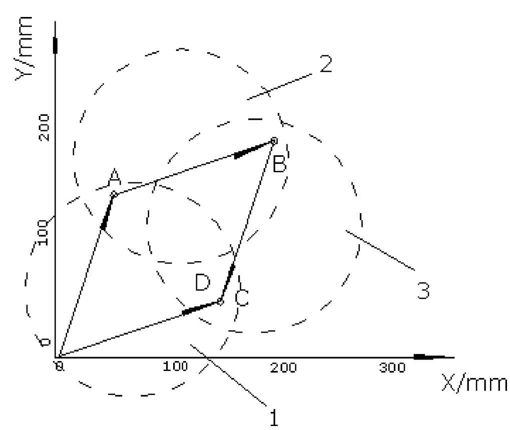

Fig. 6 Two-time relay measurements

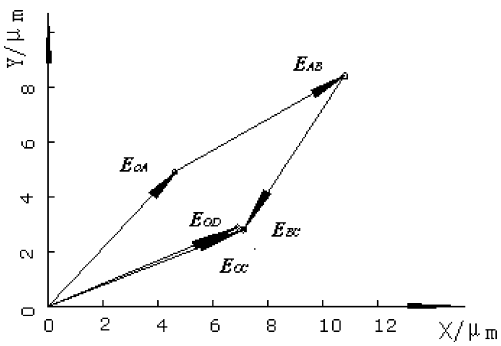

Fig. 7 Results of two-time measurements

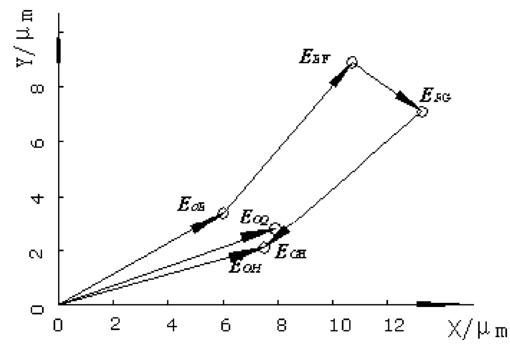

Fig. 9 Results of three-time measurements

2.6 Relay measurement method

The characteristics mentioned above have guided us in the error measurement method used in the experimental work described below. The measurement method was as follows.

1. The position errors are measured from the reference point to the end point. The reference point error can be obtained by resetting the device value to zero. For example, in Fig. 3, if the machine moves from point ***O*** to point ***A*** and then to point ***P***, the error is given by $\boldsymbol{E_{OP}}$ when the measurement device is set to zero at the point ***O***. But if the device is set to zero at the point ***A***, the error is given by $\boldsymbol{E_{AP}}$.
2. Small deviations in the reference point and end point have no effect on the error value. For example, in Fig. 5, if the measurement device is moved from point ***A*** to point ***A′***, which can happen when the device is moved on the table, the error $\boldsymbol{E_{AP}}$ equals $\boldsymbol{E_{A'P'}}$.
3. Errors in the whole workspace are mapped by measuring the error of a basic position near the original point with equipment that can measure only a small field. Then positional errors far away from the original point are measured on the basis of the first positional error. By using an analogous method, information about the positional errors of points in the entire plane can be obtained. We call this method the relay method.

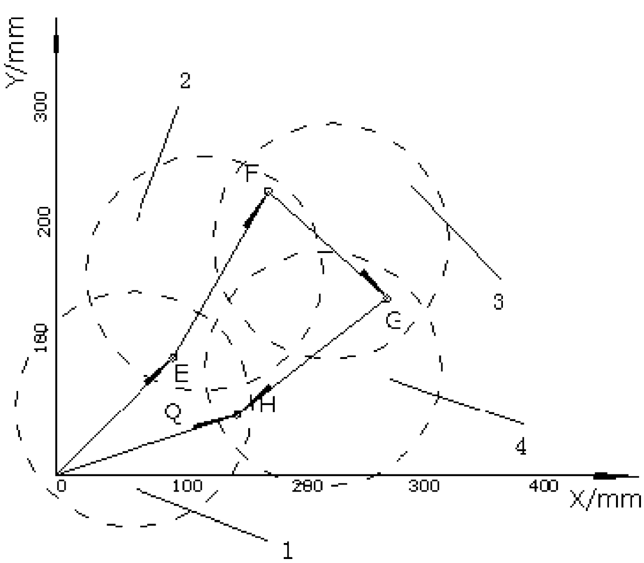

Fig. 8 Three-time relay measurements

3 Experimental procedure

In this section, we describe some tests designed to measure the characteristics mentioned above.

3.1 Experimental conditions

A new type of milling center (DM 4600, Huazhong Numerical Control Co., LTD, Wuhan, China) with three orthogonal axes was used. To avoid high-speed effects, a low feed speed (f=50 mm/min) was applied. Before the calibration was done, the X and Y axes of the milling machine were programmed to move simultaneously without actual cutting for about 3 h to eliminate the influence of temperature. The center was in a small laboratory room

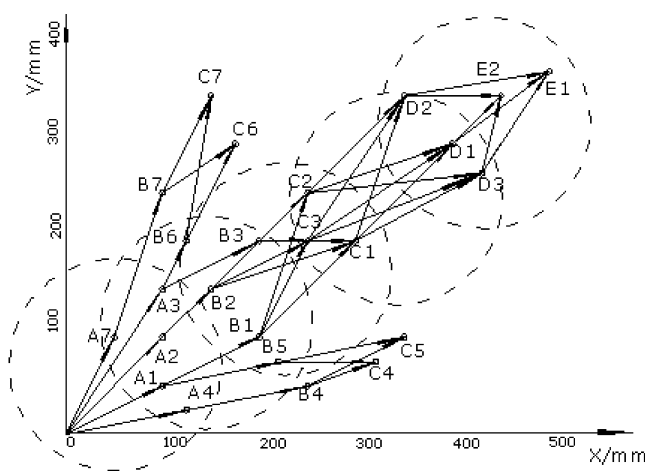

Fig. 10 Different-path error measurement

Table 1 Maximum magnitude of the difference of the error (μm)

Position	C1	C2	C3	C4	C5	C6	C7	D1	D2	D3	E1	E2
$\boldsymbol{E_X}$	0.8	0.8	0.7	0.1	0.6	0.8	0.3	1.3	1.0	0.6	0.4	0.3
$\boldsymbol{E_Y}$	0.7	1.0	1.0	0.4	0.3	0.1	0.1	1.4	1.8	1.6	2.1	1.4

without any vibration, and the backlash errors in the three axes had been well compensated. The environmental temperature was kept at 18±0.5°C during the experimental procedure. A cross-grid encoder was used to measure the two-dimensional error in a small area of the planar table. The cross-grid encoder was 220 mm in diameter with a high accuracy of 0.1 μm.

3.2 Two-time relay measurements

Figure 6 illustrates the two-time measurement procedure. The errors $\boldsymbol{E_{OA}}$ (E_{OAX}, E_{OAY}) and $\boldsymbol{E_{OD}}$ (E_{ODX}, E_{ODY}) are measured when the cross-grid encoder is in the original position (position 1). Here, E_{OAX} and E_{OAY} are the components of the error $\boldsymbol{E_{OA}}$ in the directions of the x and y-axes.

When the device is moved to position 2, the errors $\boldsymbol{E_{AB}}$ (E_{ABX}, E_{ABY}) can be obtained. The errors $\boldsymbol{E_{BC}}$ (E_{BCX}, E_{BCY}) can be obtained when the cross-grid encoder is moved to position 3. These errors were measured five times at each position. The results showed a very good repeatability of less than 1 μm. The error vectors were acquired by using the average value of the five measurements. Figure 7 shows the results for the error vectors after the two-time relay measurements.

The directly measured errors and the synthesized errors which were obtained by the two-time relay measurement procedure could also be measured in other area on the machine table. The all results obtained in this way showed a difference of less than ±0.5 μm in the x and y directions.

3.3 Three-time relay measurements

Figure 8 shows the three-time relay measurement procedure. The errors $\boldsymbol{E_{OE}}$ (E_{OEX}, E_{OEY}) and $\boldsymbol{E_{OQ}}$ (E_{OQX}, E_{OQY}) are measured when the cross-grid encoder is in the original position (position 1). Then the errors $\boldsymbol{E_{EF}}$, $\boldsymbol{E_{FG}}$ and $\boldsymbol{E_{GH}}$ are measured by moving the device to different positions. Here, the points Q and H were the same commanded point (150, 50 mm).

These errors were also measured five times in the same position. The average values of these error vectors are illustrated in Fig. 9.

The directly measured errors and the synthesized errors which were obtained by the three-time relay measurement procedure could also be measured in other area on the machine table. The all results obtained in this way showed a difference of less than ±1.0 μm in the x and y directions.

3.4 Different-path relay measurements

The influence of different paths on the error measurement was investigated as shown in Fig. 10. The errors $\boldsymbol{E_{OA1}}$, $\boldsymbol{E_{OA2}}$, $\boldsymbol{E_{OA3}}$, $\boldsymbol{E_{OA4}}$, and $\boldsymbol{E_{OA7}}$ could be obtained when the device was in the original position. The errors $\boldsymbol{E_{A1B1}}$, $\boldsymbol{E_{A1B5}}$, $\boldsymbol{E_{A2B2}}$, $\boldsymbol{E_{A3B3}}$, $\boldsymbol{E_{A3B6}}$, $\boldsymbol{E_{A4B4}}$, and $\boldsymbol{E_{A7B7}}$ were acquired after the grid encoder had been moved for the first time.

Then, after the device had been moved to several different positions, the errors $\boldsymbol{E_{B1C1}}$, $\boldsymbol{E_{B1C3}}$, $\boldsymbol{E_{B1C2}}$, $\boldsymbol{E_{B2C1}}$, $\boldsymbol{E_{B2C2}}$, $\boldsymbol{E_{B2C3}}$, $\boldsymbol{E_{B3C1}}$, $\boldsymbol{E_{B3C2}}$, $\boldsymbol{E_{B3C3}}$, $\boldsymbol{E_{B4C4}}$, $\boldsymbol{E_{B4C5}}$, $\boldsymbol{E_{B5C4}}$, $\boldsymbol{E_{B5C5}}$, $\boldsymbol{E_{B6C6}}$, $\boldsymbol{E_{B6C7}}$, $\boldsymbol{E_{B7C6}}$, $\boldsymbol{E_{B7C7}}$, $\boldsymbol{E_{C1D1}}$, $\boldsymbol{E_{C1D2}}$, $\boldsymbol{E_{C1D31}}$, $\boldsymbol{E_{C2D1}}$, $\boldsymbol{E_{C2D2}}$, $\boldsymbol{E_{C2D3}}$, $\boldsymbol{E_{C3D1}}$, $\boldsymbol{E_{C3D2}}$, $\boldsymbol{E_{C3D3}}$, $\boldsymbol{E_{D1E1}}$, $\boldsymbol{E_{D1E2}}$, $\boldsymbol{E_{D2E1}}$, $\boldsymbol{E_{D2E2}}$, $\boldsymbol{E_{D3E1}}$, and $\boldsymbol{E_{D3E2}}$ could be measured. So, the errors $\boldsymbol{E_{OC1}}$, $\boldsymbol{E_{OC2}}$, $\boldsymbol{E_{OC3}}$, $\boldsymbol{E_{OC4}}$, $\boldsymbol{E_{OC4}}$, $\boldsymbol{E_{OC6}}$, $\boldsymbol{E_{OC7}}$, $\boldsymbol{E_{OD1}}$, $\boldsymbol{E_{OD2}}$, $\boldsymbol{E_{OD3}}$, $\boldsymbol{E_{OE1}}$, and $\boldsymbol{E_{OE2}}$ for different paths could be calculated by the relay method. For example, $\boldsymbol{E_{OD1}}$ could be acquired through the relay paths $OD1 = OA1 + A1B1 + B1C1 + C1D1 = OA2 + A2B2 + B2C2 + C2D1 = OA3 + A3B3 + B3C3 + C3D1$. The maximum magnitude of the difference of the error for the different paths is given in Table 1. The maximum error in the x-axis is 1.3 μm and the maximum error in the y-axis is 2.1 μm.

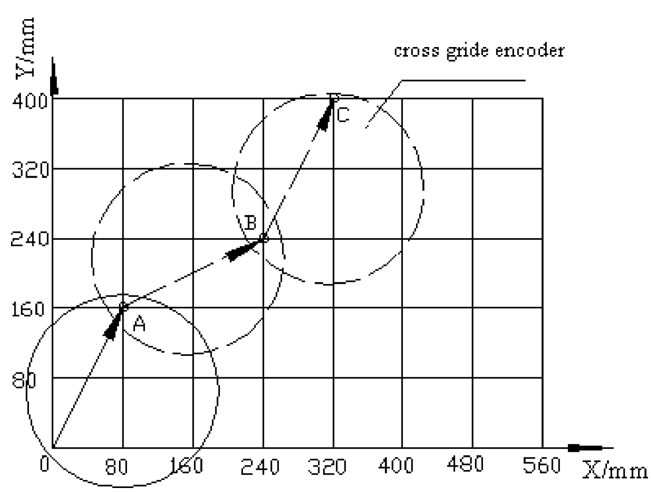

Fig. 11 Error measurement procedure

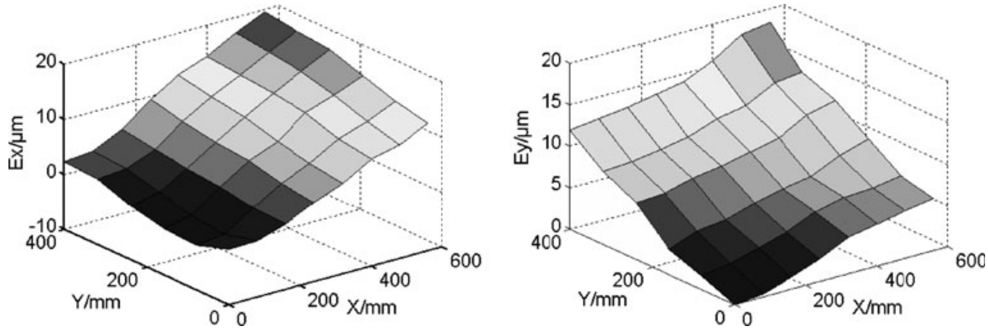

Fig. 12 Position error maps before compensation

All of the experimental results demonstrate that the systematic error increases as the number of relaying steps increases. Therefore, errors should be obtained with the smallest possible number of measurements. When the numbers of relaying steps are equal, the track of the measurement has less influence on the results. The relay method can therefore be used for the calibration of CNC machine tools.

3.5 Analysis of accumulation of errors

The position accuracy (Λ) which was measured by the relay method could be described by a positive distribution

$$\Lambda_i = \pm\sqrt{\sum_{i=1}^{t} (\alpha_i \delta_i)^2} \tag{6}$$

where α is the coefficient of error transmission, equal to 1; δ is the accuracy of the cross-grid encoder, equal to 1.5 μm; and t is the number of relaying steps in the measurement. So, Λ_2=2.6 μm, Λ_3=3.0 μm, and Λ_4=3.3 μm.

The accumulated error increases as the number of relaying steps increases. The position error should therefore be obtained with the least number of relaying steps. The position errors which need more relaying steps refer to points far away from the original point and usually have larger magnitudes. So the influence of the accumulation of errors is still in a controlled condition even when there are many relaying steps.

4 Results of error compensation

4.1 Error measurement

The position error measurement procedure that we used is shown in Fig. 11 in the *XOY* plane. In order to obtain the discrete distribution of the error vector in detail, a network of nodal points with a spacing of 80 mm was taken in the 600×400 mm workspace of the machine. The errors of the positions near to the original position were measured first. For example, for position ***A*** (80, 160), the error $\boldsymbol{E_{OA}}$ (E_{OAX}, E_{OAY}) was measured with the cross-grid in the original position. The positions measured in this way were (0, 0), (80, 0), (160, 0), (0, 80), (80, 80), (160, 80), (0, 160), and (80, 160). Then, for position ***B*** (240, 240), the error $\boldsymbol{E_{AB}}$ (E_{ABx}, E_{ABy}) was obtained based on the position ***A*** by one-time relay measurements. The error $\boldsymbol{E_{BC}}$ (E_{BCx}, E_{BCy}) was acquired by two-time relay measurements. Error information for points in the entire plane could be obtained analogously.

4.2 Error maps

The position errors of network nodes relative to the original point were acquired by the relay method. For example, for position ***B***, $E_{OB} = E_{OA} + E_{AB}$; this equation can be divided into equations for the x and y directions as follows:

$$E_{OBX} = E_{OAX} + E_{ABX} \tag{7}$$

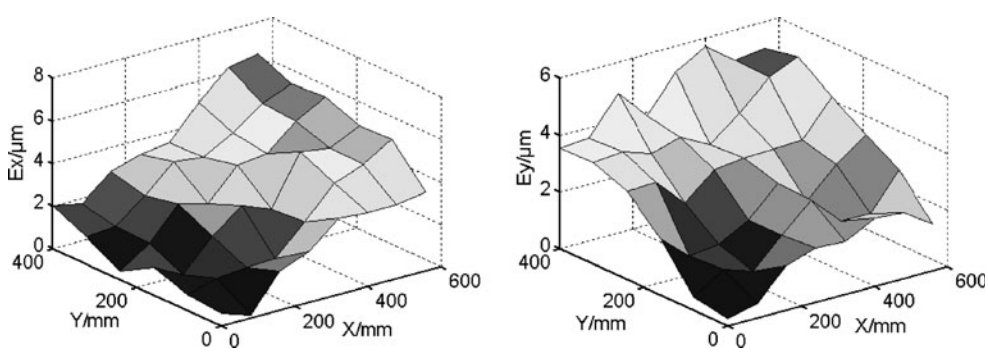

Fig. 13 Position error maps after compensation

$$E_{OBY} = E_{OAY} + E_{ABY} \tag{8}$$

The errors of the remaining positions were deduced accordingly, by the same principle. The error for position ***C*** was obtained from the equation $E_{OC} = E_{OA} + E_{AB} + E_{BC}$; this equation can be divided into

$$E_{OCX} = E_{OAX} + E_{ABX} + E_{BCX} \tag{9}$$

$$E_{OCY} = E_{OAY} + E_{ABY} + E_{BCY} \tag{10}$$

Every network position error in the x and y directions in the x–y plane was calculated in this way. The resulting error map is shown in Fig. 12, where $\boldsymbol{E_X}$ and $\boldsymbol{E_Y}$ denote the errors in the directions of the x-axis and y-axis, respectively.

These experimental results demonstrate that the method can calibrate CNC machine tools with high accuracy. The method is easy and less time-consuming than the alternatives.

4.3 Error compensation results

Calculation of the error vectors at intermediate positions was done by interpolation of the available data. As a further verification, soft error compensation was done with a Huazhong Century Star system. The results for the network node position error in the x and y directions are shown in the x–y plane in Fig. 13.

The maximum x-axis error decreased from a magnitude of 19.6 μm to 6.4 μm and the maximum y-axis error decreased from 18.4 to 5.6 μm after error compensation. The accuracy of the machine has obviously been enhanced.

5 Conclusions

From the results of this research, the following conclusions can be drawn:

1. The geometric error has the following characteristics: position dependence, relativity, synthesis, and continuity.
2. Position errors should be measured with the smallest possible number of relaying steps in order to reduce the influence of the accumulation of errors.
3. The relay method can be used as a measurement procedure for geometric errors under special conditions; the measurement operation is easy and convenient in actual applications.
4. The accuracy of the machine tool studied here was significantly enhanced after error compensation had been performed.

Acknowledgments This research was supported by the National Natural Science Federation (No. 50975053), the National Advanced Technology Plan Project (No. 20002AA423260) and the Zhanjiang Science and Technology Plan Project (No. 2008C09016). The authors also would like to thank Heidenhain Co. for free use of the KGM measurement system.

References

1. Ni J, Wu SM (1993) An on-line measurement technique for machine volumetric error compensation. ASME Trans J Eng Ind 115:85–92
2. Turyagyenda G, Hao W, Jianguo Y (2008) Progressive developmen to fanabsolute sensorless compensation system for cuttingforce-induced error. Int J Adv Manuf Tech 39:454–461. doi:10.1007/s00170-007-1239-x
3. Ramesh R, Mannnan MA, Poo AN (2000) Error compensation in machine tools—a review. Part I: geometric, cutting-force induced and fixture-dependent errors. Int J Mach Tools Manuf 40:1235–1256
4. Okafor AC, Ertekin YM (2000) Vertical machining center accuracy characteristics using laser interferometer part 1. Linear positional errors. J Mater Process Technol 105:394–406
5. Ziegert JC, Mize CD (1994) The laser ball bar: a new instrument for machine tool metrology. Precis Eng 16(4):259–267
6. Qiu H, Li Y, Li Y (2001) A new method and device for motion accuracy measurement of NC machine tools. Part 2: device error identification and trajectory measurement of general planar motions. Int J Mach Tools Manuf 41:535–554
7. Wang S-M, Ehmann KF (1999) Measurement methods for the position errors of a multi-axis machine. Part 1: principles and sensitivity analysis. Int J Mach Tools Manuf 39:951–964
8. Wang S-M, Ehmann KF (1999) Measurement methods for the position errors of a multi-axis machine. Part 2: applications and experimental results. Int J Mach Tools Manuf 39:1485–1505
9. HEIDENHAIN (2002) The operation manual. Measuring system for machine tool inspection and acceptance testing. Germany

Copyright of International Journal of Advanced Manufacturing Technology is the property of Springer Science & Business Media B.V. and its content may not be copied or emailed to multiple sites or posted to a listserv without the copyright holder's express written permission. However, users may print, download, or email articles for individual use.